



## OPEN Taurochenodeoxycholic acid as a sensitive stratification marker for HBV-associated hepatic cirrhosis status has a hepatoprotective effect

Jingyan Zeng<sup>1,3</sup>, Lijuan Wu<sup>1,3</sup>, Hao Xie<sup>1</sup>, Weiqiang Liu<sup>1</sup>, Na Shen<sup>2</sup> & Hongchun Luo<sup>1</sup>✉

**Keywords** TCDCA, Bile acids, LX-2, Chronic HBV infection, Hepatic cirrhosis

Bile acids (BAs) play a crucial role in the pathogenesis of hepatic cirrhosis, with their composition and effects varying across liver diseases with different etiologies. This study investigated the dynamic profile of BAs in HBV-associated chronic liver diseases, identify BA-based stratification markers for hepatic cirrhosis, and explore their role in fibrogenesis. Serum profiles of fifteen BAs were detected in patients with HBV-associated chronic liver diseases. The correlation between clinical parameters and these BAs were analyzed. BA effects on the secretion and inflammatory phenotype of LX-2 cells were assayed by ELISA and flow cytometry. Five conjugated BAs progressively increased during the progression of liver disease. Among them, taurochenodeoxycholic acid (TCDCA) was superior to the other BAs in evaluating the severity of hepatic cirrhosis. TCDCA was positively correlated with AFP, AST, DBIL, PT, and CysC. Effective antiviral treatment significantly reduced the level of TCDCA. Meanwhile, TCDCA stimulated IL-10 secretion and suppressed IL-15 and fibrous mediator release by LX-2 cells. It also enhanced the fluorescence intensity of IL-15R and IL-22R, while reducing IL-17R intensity on LX-2 cells. Therefore, TCDCA could serve as a promising stratification biomarker of HBV-related hepatic cirrhosis, possessing anti-inflammatory and anti-fibrotic properties that may contribute to ameliorating liver fibrosis.

Hepatitis B virus (HBV) infection continues to pose a significant global health challenge. Chronic HBV infection is characterized by suppressed innate immunity and compromised CD8+ T cell function<sup>1–3</sup>, which could subsequently progress to liver fibrosis, hepatic cirrhosis (HC), and hepatocellular carcinoma (HCC)<sup>4,5</sup>. Emerging clinical evidences have demonstrated that timely therapeutic interventions can partially reverse hepatic fibrosis and cirrhosis<sup>6–9</sup>. Therefore, identifying sensitive stratification markers of hepatic cirrhosis and novel therapeutic strategies is crucial.

BAs, as essential components of bile, serve critical functions in glycolipid metabolism<sup>10–12</sup>, immunomodulation<sup>13–15</sup>, gut microbiota homeostasis, and oncogenic processes<sup>16</sup>. Recent studies have shown that BAs are involved in the pathogenesis of hepatic cirrhosis. For instance, BAs drive the progression of nonalcoholic fatty liver disease (NAFLD) through farnesoid X receptor (FXR) and Takeda G protein-coupled receptor 5 (TGR5)-dependent signaling pathways<sup>17,18</sup>. Glycoursodeoxycholic acid exacerbates liver fibrosis by activating TGR5-mediated p38MAPK and ERK1/2 signaling cascades<sup>19</sup>. Although BA profiles exhibit distinct alterations across chronic liver diseases of various etiologies<sup>20,21</sup>, the specific patterns characterizing the transition from chronic hepatitis B (CHB) to HBV-associated compensated hepatic cirrhosis (HBV-CHC) and subsequently to HBV-associated decompensated hepatic cirrhosis (HBV-DHC) remain undefined. Furthermore, the functions of stage-specific bile acids and potential associations between BA profiles and anti-HBV therapeutic efficacy require elucidation.

This investigation characterized BA profiles across different stages of HBV-related chronic liver disease, evaluated their correlation with clinical parameters, and assessed the impact of candidate BAs on the secretion and inflammatory phenotype of hepatic stellate cells in fibrogenesis. It contributed to the identification of

<sup>1</sup>Department of Infectious Diseases, The First Affiliated Hospital of Chongqing Medical University, No. 1 Youyi Road, Yuzhong District, Chongqing 400016, China. <sup>2</sup>Department of Emergency, The First Affiliated Hospital of Chongqing Medical University, Chongqing 400016, China. <sup>3</sup>Jingyan Zeng and Lijuan Wu these equally contributions to this work. ✉email: hongchunluo@hospital.cqmu.edu.cn

BA-based stratification markers for HBV-associated hepatic cirrhosis (HBV-HC) and provided insights into therapeutic strategies targeting BA signaling in hepatic fibrogenesis.

## Materials and methods

### Subjects

In our study, all the subjects were obtained from the First Affiliated Hospital of Chongqing Medical University, China. Blood samples were collected from patients with CHB, HBV-HC, and HBV-HCC. The inclusion criterion for patients with chronic HBV infection was that the patients had a HBsAg-positive status for more than 6 months with or without a detectable HBV-DNA load. The exclusion criteria included autoimmune disorders, bacterial, fungal, or other viral infections, taking medication that interfered with the metabolism of bile acid, history of cholecystectomy, extrahepatic tumor, or any other pre-existing chronic conditions. According to Chinese guidelines on the management of liver cirrhosis from Chinese Society of Hepatology of the Chinese Medical Association, HC was diagnosed by histopathology, ultrasound and imaging features, clinical manifestations, and laboratory tests. HC was further classified into two categories: CHC and DHC. Diagnosis of HCC was confirmed by pathological changes or imaging characteristics.

All procedures were performed in accordance with the 1975 Declaration of Helsinki and the ethical standards of The First Affiliated Hospital of Chongqing Medical University (Approval No.2020 – 841).

### Bile acid assay in peripheral blood

Peripheral blood samples were collected in the early morning after fasting. Serum was promptly separated by centrifugation at 3000 rpm for 5 min. Based on the nature of the analyte, appropriate liquid chromatography conditions and mass spectrometry parameters were selected for UHPLC-HRMS analysis to determine bile acid concentrations. The concentrations of BAs including GCA, Glycochenodeoxycholic acid (GCDCA), Glycoursodeoxycholic acid (GUDCA), TCA, TCDCA, Tauroursodeoxycholic acid (TUDCA), Cholic acid (CA), Lithocholic acid (LCA), Chenodeoxycholic acid (CDCA), Ursodeoxycholic acid (UDCA), Glycolithocholic acid (GLCA), Glycodeoxycholic acid (GDCA), Tauroolithocholic acid (TLAC), Taurodeoxycholic acid (TDAC) and Deoxycholic acid (DCA) were comprehensively analyzed.

### Clinical data collection

The collected clinical data included gender, age, alpha-fetoprotein (AFP), alanine aminotransferase (ALT), aspartate aminotransferase (AST), gamma-glutamyl transpeptidase (GGT), total bilirubin (TBIL), direct bilirubin (DBIL), creatinine (Cr), blood urea nitrogen (Bun), cystatin C (CysC), prothrombin time (PT), fibrinogen (FIB), D dimer, fibrinogen degradation products (FDP), HBV-DNA load, HBsAg, HBeAg, HBeAb, and HBcAb.

### Cell stimulation

LX-2 cells, a human hepatic stellate cell line (CTCC-0373-Luc1, MeisenCTCC, CHN), were inoculated in 24-well plates at a concentration of  $5 \times 10^4$ /ml and cultured in DMEM supplemented with 2% foetal bovine serum (FBS). After cell adherence, LX-2 cells were stimulated with TCDCA at a concentration of 50  $\mu$ M, 100  $\mu$ M, 150  $\mu$ M, and 200  $\mu$ M for 24 h, 48 h, and 72 h, respectively. Simultaneously, a control group (DMSO) was established. Then, the supernatant was collected for detecting cytokines (IL-1 $\beta$ , IL-6, IL-10, IL-15, and TNF- $\alpha$ ) and fibrous markers (HA, colIV, LN, and PIIINP) by ELISA.

### Flow cytometry

LX-2 cells were cultured in 6-well plates and stimulated with 100  $\mu$ M TCDCA for 72 h. Subsequently, LX-2 cells in the experimental group and the control group were collected for flow cytometry. Anti-IL-20R, anti-IL-22R, anti-IL-15R, and anti-IL-17R were purchased from R&D systems (Wuhan, Hubei, China). The LX-2 cells were resuspended in antibody diluent and incubated for 45 min. Then, these cells were washed in PBS supplemented with 1% FBS. After washing them again, the supernatant was discarded. Finally, antibody-stained LX-2 cells were resuspended in PBS supplemented with 1% PFA. All data were analyzed using Flowjo software.

### Statistical analysis

Statistical analyses were performed using R language version 4.2.0 (<https://mirrors.tuna.tsinghua.edu.cn/CRA/N/>). When the data did not conform to a Gaussian distribution, nonparametric Kruskal-Wallis test was used to compare the differences in BAs across different groups, while Wilcoxon-Mann-Whitney test was applied for the comparison of two variables. The stratification biomarkers for HBV-associated chronic liver diseases were identified using receiver operating characteristic (ROC) curves generated by the “pROC” package Version 1.18.4 (<https://cran.r-project.org/web/packages/pROC/index.html>). The correlation between the clinical parameters and BAs was calculated by Spearman correlation analysis using the “rcorr” function in the “Hmisc” package Version 5.1-0 (<https://cran.r-project.org/web/packages/Hmisc/>). Unpaired t test was conducted to analyze the impact of TCDCA on LX-2 in cell stimulation experiment.  $P < 0.05$  was considered statistically significant.  $0.3 \leq R$  value  $< 0.5$ : weak correlation,  $0.5 \leq R$  value  $< 0.8$ : moderate correlation,  $0.8 \leq R$  value  $\leq 1$ : strong correlation.

## Results

### The dynamic alterations of fifteen BAs at different stages of chronic liver diseases associated with HBV infection

A cohort of 267 patients with chronic HBV infection was prospectively enrolled, comprising 117 CHB, 47 HBV-CHC, 49 HBV-DHC, and 54 HBV-HCC cases. Demographic and clinical characteristics of the cohort were

presented in Table 1. Quantitative analysis revealed progressive elevations in five conjugated BAs, including GCA (CHB vs. HBV-CHC:  $P=0.026$ ; HBV-CHC vs. HBV-DHC:  $P=0.001$ ), GCDCA (CHB vs. HBV-CHC:  $P=0.023$ ; HBV-CHC vs. HBV-DHC:  $P=2.2e-08$ ), TCA (CHB vs. HBV-CHC:  $P=0.0018$ ; HBV-CHC vs. HBV-DHC:  $P=7.2e-10$ ), TCDCA (CHB vs. HBV-CHC:  $P=8.7e-05$ ; HBV-CHC vs. HBV-DHC:  $P=5.1e-09$ ), and TUDCA (CHB vs. HBV-CHC:  $P=0.0035$ ; HBV-CHC vs. HBV-DHC:  $P=3.4e-06$ ), from the CHB to the HBV-CHC and the HBV-DHC, with TCDCA showing the most pronounced dynamic changes. Concurrently, DCA ( $P=0.026$ ) and LCA ( $P=0.011$ ) concentrations were significantly reduced from the HBV-CHC to the HBV-DHC, although no intergroup differences were observed between the CHB and HBV-CHC groups (Fig. 1A). ROC curve analysis identified TCDCA as a robust diagnostic biomarker, with optimal cutoff values of 101.08 ng/ml for distinguishing CHB from HBV-CHC (AUC 0.7677, Youden index 0.4445, sensitivity 0.7778, specificity 0.6667, 95%IC: 0.6570–0.8783) (Fig. 1B) and 1588.6 ng/ml for distinguishing HBV-CHC from HBV-DHC (AUC 0.8030, Youden index 0.5698, sensitivity 0.7872, specificity 0.7826, 95%IC: 0.7125–0.8934) (Fig. 1C). Compared with the established non-invasive fibrosis biomarkers, such as APRI, FIB-4, and GPR, TCDCA exhibited superior diagnostic accuracy for HBV-CHC (Fig. S1A). For HBV-DHC, its diagnostic performance was only marginally lower than that of FIB-4, while outperforming these of APRI and GPR (Fig. S1B). In addition, our data revealed that the level of UDCA ( $p=0.036$ ) is elevated in the HBV-HCC group compared to that in the HBV-related benign liver disease group (Fig. S1C).

### The correlations between these five conjugated BAs and the clinical parameters in patients with chronic HBV infection

To explore the clinical significance of five conjugated BAs in the progression of chronic HBV infection, we analyzed their correlations with immunological, biochemical, and virological markers. The results revealed that AFP was positively correlated with GCA (CHB:  $R=0.4400$ ,  $P<0.0001$ ; HBV-HC:  $R=0.5440$ ,  $P<0.0001$ ), GCDCA (CHB:  $R=0.3750$ ,  $P<0.001$ ; HBV-HC:  $R=0.4590$ ,  $P<0.0001$ ), TCA (CHB:  $R=0.5010$ ,  $P<0.0001$ ; HBV-HC:  $R=0.6040$ ,  $P<0.0001$ ), TCDCA (CHB:  $R=0.4590$ ,  $P<0.0001$ ; HBV-HC:  $R=0.5510$ ,  $P<0.0001$ ), and TUDCA (CHB:  $R=0.4550$ ,  $P<0.0001$ ; HBV-HC:  $R=0.4550$ ,  $P<0.0001$ ) in both the CHB and HBV-HC groups. Notably, the correlations of AFP with GCA and TCDCA were stronger in the HBV-HC group compared to the CHB group (Fig. 2A).

Further correlation analysis between liver function parameters and the five conjugated BAs demonstrated positive correlations of AST, ALT, DBIL, and GGT with four conjugated BAs, including GCA, GCDCA, TCA, and TCDCA, in both the CHB and HBV-HC groups. Moreover, the correlations of these four conjugated BAs with AST and DBIL were stronger in the HBV-HC group compared to the CHB group (Fig. 2B–E). However, a positive correlation with TBIL was observed only in the HBV-HC group (Fig. 2F).

Regarding the effects of these five conjugated BAs on coagulation function, our data indicated a positive correlation with PT. Among these, TCDCA showed a weak correlation with PT in the CHB ( $R=0.4420$ ,  $P<0.01$ ) and a moderate correlation with PT in the HBV-HC ( $R=0.5390$ ,  $P<0.0001$ ) (Fig. 2G). No correlations were observed between these five conjugated BAs and D-dimer, FDP, or FIB (Fig. S2 A–C).

Clinical parameters	HBV-CHB (n=117)	HBV-CHC (n=47)	HBV-DHC (n=49)	HBV-HCC (n=54)
Age(year)	39 (30, 49)	48 (37.50, 53.00)	57 (51, 66)	54 (49, 62)
Gender (male/female)	81/36	36/11	31/18	41/13
AFP (ng/ml)	3.55 (2.48, 6.75)	5.20 (2.70, 22.30)	8.85 (2.63, 61.95)	247.8 (6.20, 2537.50)
ALT (U/L)	31.00 (20.00, 75.00)	38.45 (20.25, 86.50)	36.00 (21.00, 74.00)	34.00 (23.25, 60.25)
AST (U/L)	23.00 (18.00, 46.00)	32.00 (21.00, 56.50)	52.00 (30.00, 116.00)	50.00 (29.25, 123.00)
GGT (U/L)	23.00 (15.00, 64.50)	36.00 (21.00, 92.00)	47.00 (21.50, 126.00)	122.00 (37.50, 276.00)
TBIL (umol/L)	11.90(9.70,16.40)	15.65(12.30,35.27)	41.30(20.80,78.40)	25.10(13.78,47.10)
DBIL(umol/L)	4.70(3.70,6.70)	7.30(4.93,12.83)	14.70(6.60,51.80)	10.05(5.00,24.12)
BUN (mmol/L)	4.40(3.60,5.40)	4.55(3.70,5.78)	5.20(4.30,6.30)	5.60(3.83,7.45)
Cr (umol/L)	75.00(62.50,82.50)	73.00(61.25,86.00)	70.00(60.00,88.00)	69.50(56.25,78.75)
Cysc (mg/L)	0.75(0.64,0.84)	0.90(0.77,1.00)	1.22(1.05,1.45)	0.90(0.79,1.16)
PT (s)	13.70(13.20,14.30)	14.30(13.40,16.00)	17.35(15.78,18.82)	14.90(14.00,16.20)
FIB (g/L)	2.10(1.81,2.61)	2.17(1.85,2.47)	2.01(1.57,2.45)	2.49(2.10,3.89)
FDP (μg/ml)	0.85(0.60,1.68)	0.90(0.60,1.20)	4.55(2.45,10.45)	3.10(0.70,8.90)
D dimer (mg/L)	0.35(0.16,0.49)	0.24(0.17,0.34)	1.63(0.91,4.38)	1.27(0.50,3.54)
HBV-DNA (log <sub>10</sub> IU/ml)	1.90(1.28,4.43)	1.28(1.28,6.15)	2.89(1.28,4.05)	2.06(1.28,4.19)
HBsAg (IU/ml)	2090.60 (430.10,5263.30)	1612.00 (258.80,4561.00)	289.00 (95.33,1125.30)	732.81 (84.99,1975.87)
HBeAg (S/CO)	0.51(0.38,108.11)	0.50(0.35,8.51)	0.37(0.06,0.48)	0.36(0.05,0.74)
HBeAb (S/CO)	1.02(0.02,19.43)	0.72(0.02,19.60)	0.30(0.02,90.66)	1.56(0.03,95.51)
HBcAb (S/CO)	8.54(7.98,9.40)	9.02(8.24,9.90)	10.97(8.55,476.26)	9.56(8.48,392.16)

**Table 1.** Demographic and clinical characteristics of the cohort.

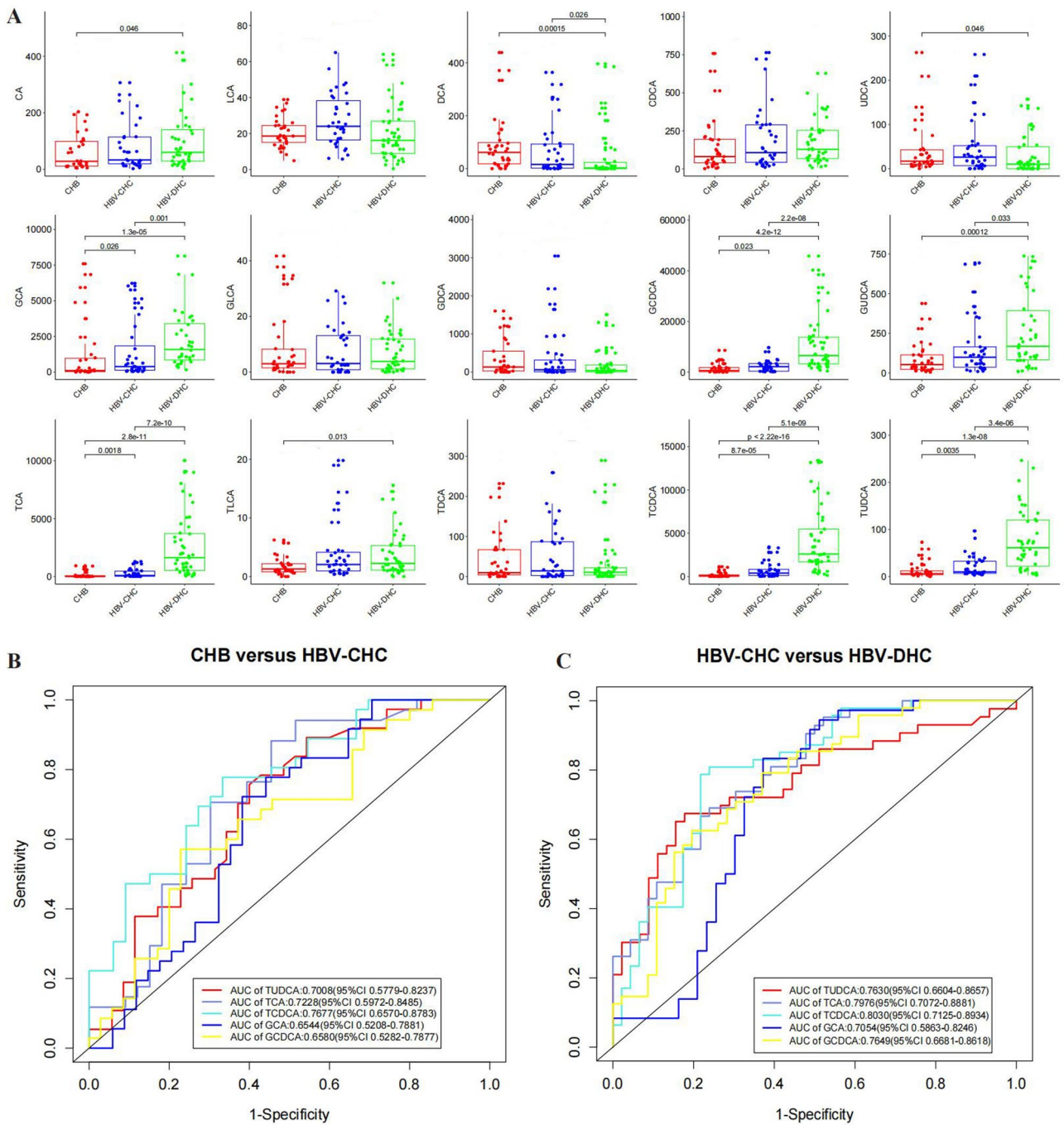


**Fig. 1.** Progressive increase in the levels of five conjugated BAs during the progression of HBV-associated chronic liver diseases and their potential for assessing hepatic cirrhosis. **A.** The levels of GCA, GCDCA, TCA, TCDCA, and TUDCA were progressively elevated from the CHB to the HBV-CHC and to the HBV-DHC group. **B.** ROC curve analysis indicated that TCDCA could effectively differentiate the CHB from the HBV-CHC. **C.** TCDCA showed potential for distinguishing the HBV-CHC from the HBV-DHC. The horizontal bars represent the median, and the extremities of the vertical bars represent the range (25%–75% in the scatter dot plot).

Additionally, the correlation analysis between the five conjugated BAs and renal function revealed that GCDCA (CHB:  $R=0.3360$ ,  $P<0.001$ ; HBV-HC:  $R=0.3770$ ,  $P<0.001$ ), TCA (CHB:  $R=0.4040$ ,  $P<0.0001$ ; HBV-HC:  $R=0.3260$ ,  $P<0.01$ ), and TCDCA (CHB:  $R=0.3980$ ,  $P<0.0001$ ; HBV-HC:  $R=0.3900$ ,  $P<0.001$ ) are positively correlated with CysC in both the CHB and HBV-HC groups (Fig. 2H). Notably, TCDCA exhibited the strongest positive correlation with CysC. However, no correlation was observed between these BAs and Cr or BUN (Fig. S2 D.E). These findings suggested that TCDCA may serve as an indicator for early kidney injury.

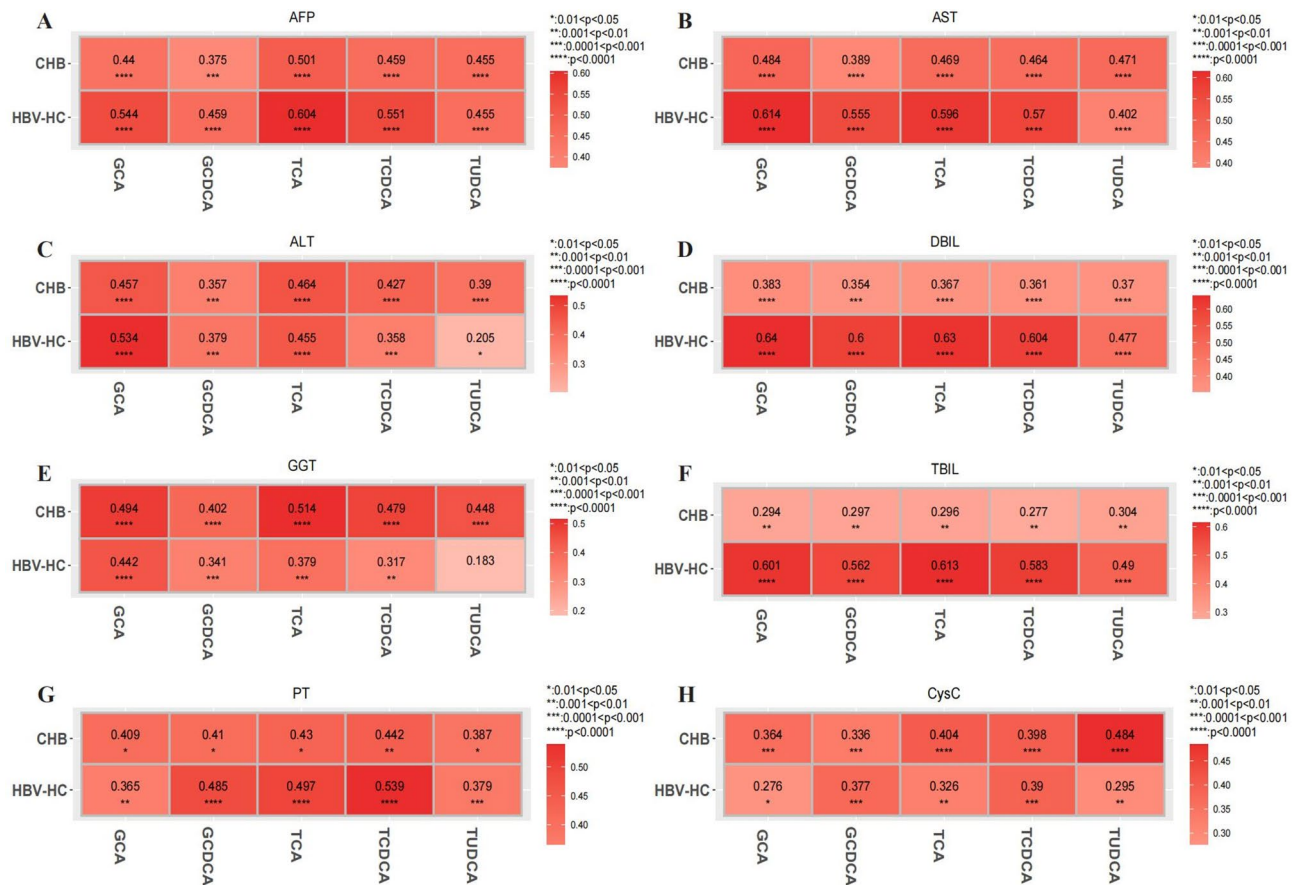


**Fig. 2.** Correlation of five conjugated BAs with some clinical indicators in HBV-associated chronic liver diseases. A. Five conjugated BAs were positively correlated with AFP. B–E. GCA, GCDCA, TCA, and TCDCA were positively associated with AST, ALT, DBIL, and GGT in the CHB and the HBV-HC. F. GCA, GCDCA, TCA, and TCDCA were only positively correlated with TBIL in the HBV-HC. G. These 5 conjugated BAs have a positive correlation with PT. H. GCDCA, TCA, and TCDCA were positively correlated with CysC.

In patients receiving antiviral treatment, we compared the serum levels of five conjugated BAs between two groups: one with an HBV-DNA load  $< 20$  IU/L (antiviral-low) and the other with an HBV-DNA load  $\geq 20$  IU/L (antiviral-high). The data revealed a significant decrease in the levels of GCA ( $P = 0.016$ ) and TCDCA ( $P = 0.027$ ) in the antiviral-low CHB group compared to the antiviral-high CHB group (Fig. 3A). Similarly, in the antiviral-low HBV-HC group, we observed significantly reduced levels of GCA ( $P = 9.2e-06$ ), GCDCA ( $P = 0.00058$ ), TCA ( $P = 0.0015$ ), and TCDCA ( $P = 0.0088$ ) compared to the antiviral-high HBV-HC group (Fig. 3B). These findings suggested that effective antiviral treatment can significantly lower the levels of GCA and TCDCA in both the CHB and HBV-HC groups, with a more pronounced effect in the antiviral-low HBV-HC group.

### The impact of TCDCA on the secretion of LX-2

To investigate the effect of TCDCA on LX-2 cells, we assayed the concentrations of some cytokines and fibrotic components in the supernatant at 24 h, 48 h, and 72 h post-stimulation. The results demonstrated that TCDCA could stimulate the secretion of IL-10 (50  $\mu\text{m}$ ,  $P = 0.0068$ ; 100  $\mu\text{m}$ ,  $P = 0.0041$ ; 150  $\mu\text{m}$ ,  $P = 0.0095$ ; 200  $\mu\text{m}$ ,  $P = 0.0093$ ), while inhibiting the secretion of IL-15 (50  $\mu\text{m}$ ,  $P < 0.0001$ ; 100  $\mu\text{m}$ ,  $P < 0.0001$ ; 150  $\mu\text{m}$ ,  $P < 0.0001$ ; 200  $\mu\text{m}$ ,  $P < 0.0001$ ) at 72 h post-stimulation (Fig. 3C). Meanwhile, TCDCA markedly suppressed the secretion of HA (50  $\mu\text{m}$ ,  $P < 0.0001$ ; 100  $\mu\text{m}$ ,  $P < 0.0001$ ; 150  $\mu\text{m}$ ,  $P < 0.0001$ ; 200  $\mu\text{m}$ ,  $P < 0.0001$ ) at 24 h post-stimulation and significantly reduced the secretion of ColIV and PIIINP at all three time points (Fig. 3D). However, there were no differences in the concentrations of IL-1 $\beta$ , IL-6, TNF- $\alpha$ , and LN between the TCDCA-stimulated group and the control group.

### The impact of TCDCA on the inflammatory phenotype of LX-2

To investigate the effect of TCDCA on the inflammatory phenotype of LX-2 cells, we detected the fluorescence intensity of IL-17R, IL-20R, IL-15R, and IL-22R in the TCDCA-stimulated group, the DMSO control group, and the isotype control group using flow cytometry. Our findings showed that the fluorescence intensity of IL-17R in the TCDCA-stimulated group is obviously decreased ( $P = 0.0392$ ), while the fluorescence intensity of IL-15R ( $P = 0.0014$ ) and IL-22R ( $P = 0.0155$ ) is significantly increased compared with that in the DMSO control group.

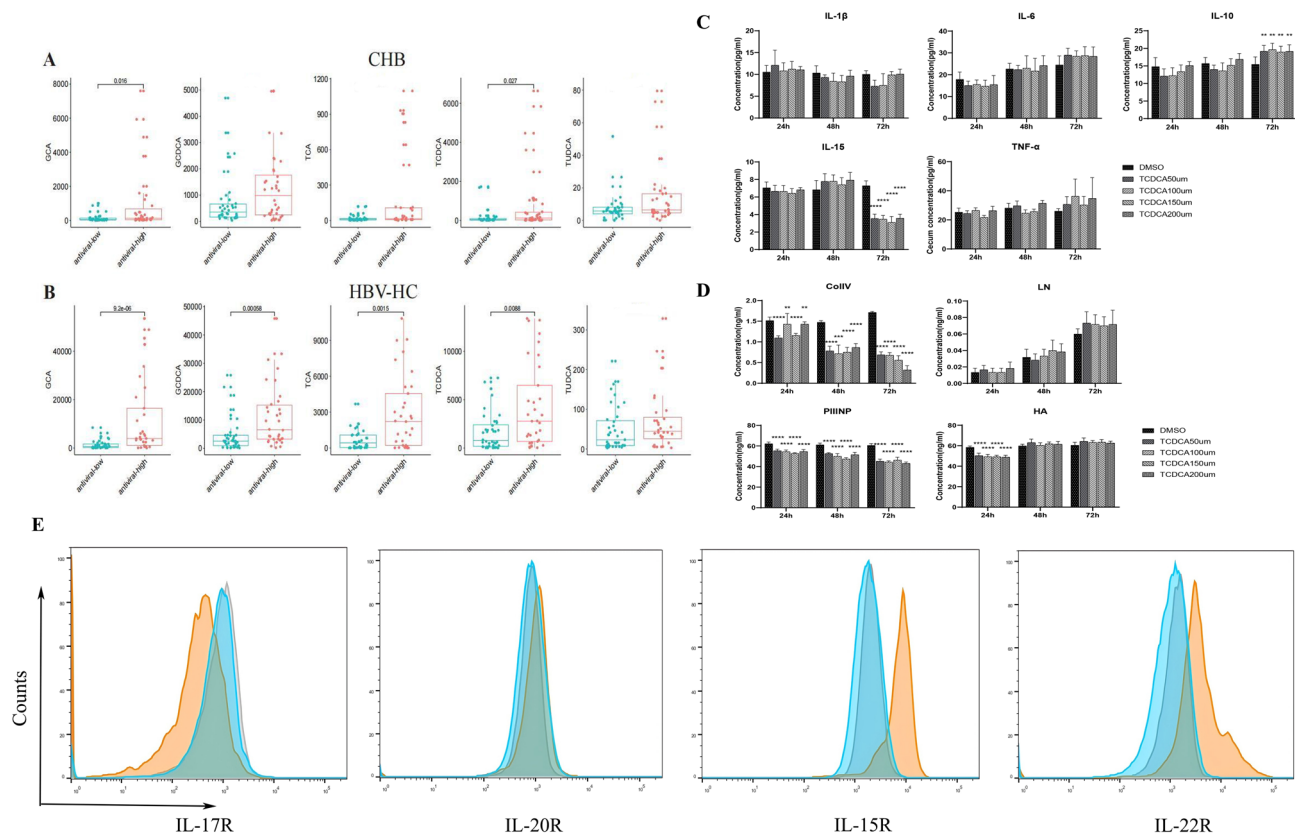


**Fig. 3.** The correlation of antiviral treatment with TCDCA and the effects of TCDCA on the inflammatory phenotype of LX-2 cells. **A.** The levels of GCA and TCDCA were significantly decreased in the antiviral-low CHB group compared to those in the antiviral-high CHB group. **B.** The levels of GCA, GCDCA, TCA, and TCDCA were significantly reduced in the antiviral-low HC group compared to those in the antiviral-high HC group. **C.** TCDCA promoted the secretion of IL-10 while inhibiting the secretion of IL-15 at 72h post-stimulation. **D.** TCDCA suppressed the secretion of HA at 24h post-stimulation and significantly reduced the secretion of ColIV and PIIINP at all three time points. **E.** TCDCA inhibited the expression of IL-17R while promoting the expression of IL-15R and IL-22R on the LX-2 cells. Fluorescence intensity in the DMSO control group and the isotype control group was represented by gray and by blue, respectively, while the fluorescence intensity in the TCDCA-stimulated group was represented by orange.

and the isotype control group. Additionally, no significant difference in the fluorescence intensity of IL-20R was observed between the TCDCA-stimulated group and the control group (Fig. 3E).

## Discussion

Liver diseases associated with HBV infection rank among the top 15 leading causes of death worldwide. Multiple factors are involved in the pathogenesis of HBV-associated chronic liver diseases. Recently, the effect of BAs on the progression of liver diseases has garnered more attention. BAs act as signaling molecules, influencing multiple physiological processes, including host energy metabolism<sup>22,23</sup> cancer progression<sup>24</sup> and immune modulation<sup>22,25,26</sup>. Some studies have shown that the profiles of BAs differ among patients with different chronic liver diseases<sup>27,28</sup>. For example, taurine conjugated bile acids are predominant in alcoholic liver diseases, while UDCA is more prevalent in primary biliary cholangitis. As for the patients with HBV infection, it has been reported that deoxycholate is the most abundant in the serum. However, our data showed that five conjugated BAs, including GCA, GCDCA, TCA, TCDCA and TUDCA, are gradually increased from CHB to HBV-CHC and to HBV-DHC, which highlights the dynamic alteration in the BA profile during the progression of liver disease. Among them, TCDCA proved to be an effective indicator for differentiating CHB from HBV-CHC, with a cutoff value of 101.08, and for identifying HBV-DHC, with a cutoff value of 1588.6. Compared to established non-invasive biomarkers for cirrhosis, such as APRI, FIB-4, and GPR, TCDCA exhibited superior diagnostic accuracy for cirrhosis, especially for HBV-CHC.

Our findings also indicated that no significant elevation in TCDCA levels was observed in the HBV-HCC group compared to the HBV-related benign liver diseases, which is consistent with previous study<sup>29</sup>. Regarding the reasons, we propose that both hepatic cirrhosis and hepatocellular carcinoma are associated with disruptions in bile acid homeostasis. As hepatocellular carcinoma develops, bile acid metabolism is extensively altered due to severe liver dysfunction, tumor-induced alterations in bile acid transporters, and shifts in gut microbiota composition<sup>30</sup>. These factors may influence altered hepatic synthesis and circulation of TCDCA. However,

UDCA elevation was found in the HBV-HCC group, which suggests potential oncogenic properties, warranting investigation into its role in hepatocarcinogenesis.

TCDCA is synthesized in liver through the conjugation of taurine and ursodeoxycholic acid<sup>31</sup> and exhibits a wide range of effects, including anti-inflammatory, anti-tumor, lipid-regulating, and immune-modulating properties. It has been reported that TCDCA is correlated with some clinical indexes such as TBIL and PT in liver diseases, especially in drug induced liver injury<sup>32</sup> and alcoholic cirrhosis<sup>33</sup>. Nevertheless, there are few studies focused on patients with chronic HBV infection. Our study provided further evidence that TCDCA is positively correlated with AFP, AST, DBIL, PT, and CysC in the CHB and the HBV-HC group. Notably, the correlations of TCDCA with AFP, AST, DBIL, and PT were more pronounced in the HBV-HC group compared to the CHB group. AFP is a well-established biomarker for liver fibrosis, inflammation and hepatocellular carcinoma<sup>34,35</sup> while the elevations of AST and DBIL indicate hepatocellular damage and cholestasis, respectively. Prolonged PT is often associated with more severe liver injury or hepatic cirrhosis, leading to impaired liver synthetic function<sup>36</sup>. Given that TCDCA plays a crucial role in the modulation of bile acid homeostasis<sup>37</sup> and hepatic inflammation<sup>38,39</sup>, the enhanced correlation of TCDCA with these parameters in the HBV-HC group suggests that TCDCA might serve as a potential biomarker for monitoring the severity of liver injury and cirrhosis. Moreover, TCDCA was positively correlated with CysC, a sensitive marker for kidney injury<sup>40–44</sup> indicating that TCDCA might also reflect early kidney injury in HBV-associated liver diseases.

Effective antiviral treatment for chronic HBV infection has been shown to significantly improve hepatic inflammation, which is also modulated by BAs. However, the impact of antiviral treatment on BA profile has remained unclear. Therefore, we analyzed the alterations of these five conjugated BAs following effective antiviral treatment. Our findings showed that the effective antiviral treatment could significantly reduce the levels of GCA and TCDCA in the CHB group, which are more pronounced in the HC group. We supposed the possible mechanisms as follow. Sodium taurocholate co-transporting polypeptide (NTCP) is a HBV cell entry receptor<sup>45</sup>. HBV competes with BAs for cellular entry. With fewer viruses entering hepatocytes due to antiviral treatment, more BAs are transported into hepatocytes through a negative feedback process. This leads to a decrease in serum BA levels and an increase in intrahepatic BA pool, accompanied by an alteration of FXR expression that is involved in HBV transcription and replication<sup>46,47</sup>. Furthermore, effective antiviral treatment reduces the secretion of inflammatory cytokines, chemokines, and other factors that drive liver fibrosis, subsequently, inhibiting cholangiocyte proliferation and periportal fibrosis<sup>48,49</sup> while ameliorating histopathological alterations. These changes help restore the BA homeostasis.

To further investigate the role of TCDCA in chronic liver diseases, we examined the levels of inflammatory cytokines, fibrotic components, and the inflammatory phenotype of LX-2 upon TCDCA stimulation. Our results demonstrated that TCDCA significantly induces the secretion of anti-inflammatory cytokine IL-10, while simultaneously suppressing the release of pro-inflammatory cytokine IL-15<sup>50</sup> and fibrotic components such as HA, ColIV, and PIIINP by LX-2 cells. Furthermore, TCDCA promoted the expression of anti-inflammatory and anti-fibrotic receptors, including IL-15R<sup>51</sup> and IL-22R<sup>52</sup> and inhibiting the expression of pro-inflammatory receptor IL-17R<sup>53</sup> on LX-2. Therefore, these findings suggested that TCDCA could possess anti-inflammatory and anti-fibrotic properties by the modulation of the secretory function and inflammatory phenotype of LX-2 cells, contributing to the hepatoprotective effect. Similarly, Li L et al. also reported that TCDCA has therapeutic potential by inhibiting the transcription and expression of AP-1<sup>54</sup>, exerting anti-inflammatory and immunomodulatory effects that may counteract fibrotic processes. Nevertheless, the precise intracellular signaling pathways mediated by TCDCA has remained unclear. Consequently, further investigation should be performed to identify the specific TCDCA-binding receptors on LX-2 cells and its down-stream signal molecules.

Our study has some limitations. This study was conducted on a relatively small cohort, which may introduce a certain degree of bias into our conclusions. Therefore, larger and multi-center cohort studies are necessary to enhance the reliability of our findings. Additionally, the molecular mechanisms by which TCDCA ameliorates liver inflammation and cirrhosis have not yet been fully elucidated. Given the intricate role of BAs in HBV-related liver diseases, further research into the interactions between TCDCA and its receptors, the downstream signaling molecules, and its efficacy in combination with existing antiviral therapies is warranted.

In conclusion, our data suggested that TCDCA could serve as a stratification marker for assessing hepatic cirrhosis. Furthermore, it not only reflected the severity of liver injury, but also act as an early indicator of kidney dysfunction. Importantly, effective antiviral treatment significantly reduced serum level of TCDCA, which could be attributed to the modulation of BA homeostasis. Moreover, we noted that TCDCA exerts anti-inflammatory and anti-fibrotic effects by modulating the inflammatory phenotype and the secretion of LX-2 cell, providing a novel therapeutic strategy targeting TCDCA signaling in hepatic fibrogenesis.

## Data availability

All data generated or analyzed during this study are included in the manuscript and supplementary information files.

Received: 27 May 2025; Accepted: 14 August 2025

Published online: 20 August 2025

## References

1. Yu, L., Guan, Y., Li, L., Lu, N. & Zhang, C. The transcription factor Eomes promotes expression of inhibitory receptors on hepatic CD8(+) T cells during HBV persistence. *FEBS J.* **289**, 3241–3261. <https://doi.org/10.1111/febs.16342> (2022).
2. Tsai, K. N., Kuo, C. F. & Ou, J. J. Mechanisms of hepatitis B virus persistence. *Trends Microbiol.* **26**, 33–42. <https://doi.org/10.1016/j.tim.2017.07.006> (2018).

3. Kennedy, P. T. F., Litwin, S., Dolman, G. E., Bertolotti, A. & Mason, W. S. Immune tolerant chronic hepatitis B: the unrecognized risks. *Viruses* **9** <https://doi.org/10.3390/v9050096> (2017).
4. Iloeje, U. H., Yang, H. I. & Chen, C. J. Natural history of chronic hepatitis B: what exactly has REVEAL revealed? *Liver Int.* **32**, 1333–1341. <https://doi.org/10.1111/j.1478-3231.2012.02805.x> (2012).
5. Pan, C. Q. & Zhang, J. X. Natural history and clinical consequences of hepatitis B virus infection. *Int. J. Med. Sci.* **2**, 36–40. <https://doi.org/10.7150/ijms.2.36> (2005).
6. Sanyal, A. J. et al. Cirrhosis regression is associated with improved clinical outcomes in patients with nonalcoholic steatohepatitis. *Hepatology* **75**, 1235–1246. <https://doi.org/10.1002/hep.32204> (2022).
7. Lo, R. C. & Kim, H. Histopathological evaluation of liver fibrosis and cirrhosis regression. *Clin. Mol. Hepatol.* **23**, 302–307. <https://doi.org/10.3350/cmh.2017.0078> (2017).
8. Kong, Y. et al. Early steep decline of liver stiffness predicts histological reversal of fibrosis in chronic hepatitis B patients treated with Entecavir. *J. Viral Hepat.* **26**, 576–585. <https://doi.org/10.1111/jvh.13058> (2019).
9. Tsuchida, T. & Friedman, S. L. Mechanisms of hepatic stellate cell activation. *Nat. Rev. Gastroenterol. Hepatol.* **14**, 397–411. <https://doi.org/10.1038/nrgastro.2017.38> (2017).
10. Xie, C. et al. Role of bile acids in the regulation of food intake, and their dysregulation in metabolic disease. *Nutrients* **13** <https://doi.org/10.3390/nu13041104> (2021).
11. Cai, J., Rimal, B., Jiang, C., Chiang, J. Y. L. & Patterson, A. D. Bile acid metabolism and signaling, the microbiota, and metabolic disease. *Pharmacol. Ther.* **237**, 108238. <https://doi.org/10.1016/j.pharmthera.2022.108238> (2022).
12. Ahmad, T. R. & Haeusler, R. A. Bile acids in glucose metabolism and insulin signalling - mechanisms and research needs. *Nat. Rev. Endocrinol.* **15**, 701–712. <https://doi.org/10.1038/s41574-019-0266-7> (2019).
13. Zhu, C. et al. 24-Norursodeoxycholic acid reshapes immunometabolism in CD8(+) T cells and alleviates hepatic inflammation. *J. Hepatol.* **75**, 1164–1176. <https://doi.org/10.1016/j.jhep.2021.06.036> (2021).
14. Hang, S. et al. Bile acid metabolites control T(H)17 and T(reg) cell differentiation. *Nature* **576**, 143–148. <https://doi.org/10.1038/s41586-019-1785-z> (2019).
15. Devlin, A. S. & Fischbach, M. A. A biosynthetic pathway for a prominent class of microbiota-derived bile acids. *Nat. Chem. Biol.* **11**, 685–690. <https://doi.org/10.1038/nchembio.1864> (2015).
16. Wu, L. et al. The gut microbiome-bile acid axis in hepatocarcinogenesis. *Biomed. Pharmacother.* **133**, 111036. <https://doi.org/10.1016/j.biopha.2020.111036> (2021).
17. Jiao, N. et al. Suppressed hepatic bile acid signalling despite elevated production of primary and secondary bile acids in NAFLD. *Gut* **67**, 1881–1891. <https://doi.org/10.1136/gutjnl-2017-314307> (2018).
18. Ding, L. et al. Vertical sleeve gastrectomy activates GPBAR-1/TGR5 to sustain weight loss, improve fatty liver, and remit insulin resistance in mice. *Hepatology* **64**, 760–773. <https://doi.org/10.1002/hep.28689> (2016).
19. Xie, G. et al. Conjugated secondary 12 $\alpha$ -hydroxylated bile acids promote liver fibrogenesis. *EBioMedicine* **66**, 103290. <https://doi.org/10.1016/j.ebiom.2021.103290> (2021).
20. Sang, C. et al. Bile acid profiles are distinct among patients with different etiologies of chronic liver disease. *J. Proteome Res.* **20**, 2340–2351. <https://doi.org/10.1021/acs.jproteome.0c00852> (2021).
21. Sugita, T. et al. Analysis of the serum bile acid composition for differential diagnosis in patients with liver disease. *Gastroenterol. Res. Pract.* **2015** (717431). <https://doi.org/10.1155/2015/717431> (2015).
22. Zhang, Z. et al. Hyocholic acid retards renal fibrosis by regulating lipid metabolism and inflammatory response in a sheep model. *Int. Immunopharmacol.* **122**, 110670. <https://doi.org/10.1016/j.intimp.2023.110670> (2023).
23. Castellanos-Jankiewicz, A. et al. Hypothalamic bile acid-TGR5 signaling protects from obesity. *Cell Metab.* **33**, 1483–1492 e1410, (2021). <https://doi.org/10.1016/j.cmet.2021.04.009>
24. Sarkar, J. et al. Conjugated bile acids accelerate progression of pancreatic cancer metastasis via S1PR2 signaling in cholestasis. *Ann. Surg. Oncol.* **30**, 1630–1641. <https://doi.org/10.1245/s10434-022-12806-4> (2023).
25. Lv, L. et al. Tauroursodeoxycholic acid alleviates trinitrobenzene sulfonic acid induced ulcerative colitis via regulating Th1/Th2 and Th17/Treg cells balance. *Life Sci.* **318**, 121501. <https://doi.org/10.1016/j.lfs.2023.121501> (2023).
26. Li, W. et al. A bacterial bile acid metabolite modulates T(reg) activity through the nuclear hormone receptor NR4A1. *Cell Host Microbe* **29**, 1366–1377 e1369, (2021). <https://doi.org/10.1016/j.chom.2021.07.013>
27. Ciocan, D. et al. Bile acid homeostasis and intestinal dysbiosis in alcoholic hepatitis. *Aliment. Pharmacol. Ther.* **48**, 961–974. <https://doi.org/10.1111/apt.14949> (2018).
28. Wang, X. et al. Serum bile acids are associated with pathological progression of hepatitis B-Induced cirrhosis. *J. Proteome Res.* **15**, 1126–1134. <https://doi.org/10.1021/acs.jproteome.5b00217> (2016).
29. Dai, S. et al. Alteration of serum bile acid profiles of HBV-related hepatocellular carcinoma identified by LC-MS/MS. *J. Cancer Res. Clin. Oncol.* **150**, 157. <https://doi.org/10.1007/s00432-024-05686-6> (2024).
30. Ma, C. et al. Gut microbiome-mediated bile acid metabolism regulates liver cancer via NKT cells. *Science* **360** <https://doi.org/10.1126/science.aan5931> (2018).
31. Zhang, Y. & Klaassen, C. D. Effects of feeding bile acids and a bile acid sequestrant on hepatic bile acid composition in mice. *J. Lipid Res.* **51**, 3230–3242. <https://doi.org/10.1194/jlr.M007641> (2010).
32. Tian, Q. et al. A High Serum Level of Taurocholic Acid Is Correlated With the Severity and Resolution of Drug-induced Liver Injury. *Clin Gastroenterol Hepatol* **19**, 1009–1019 e1011, (2021). <https://doi.org/10.1016/j.cgh.2020.06.067>
33. Xu, Y. F. et al. Difference and clinical value of metabolites in plasma and feces of patients with alcohol-related liver cirrhosis. *World J. Gastroenterol.* **29**, 3534–3547. <https://doi.org/10.3748/wjg.v29.i22.3534> (2023).
34. Yang, K., Pan, Y., Liu, L., Sun, B. & Shi, W. Serum Alpha-Fetoprotein as a predictor of liver fibrosis in HBeAg-Positive chronic hepatitis B patients. *Med. (Kaunas)*. **59**. <https://doi.org/10.3390/medicina59050923> (2023).
35. Liu, Y. R. et al. Alpha-fetoprotein level as a biomarker of liver fibrosis status: a cross-sectional study of 619 consecutive patients with chronic hepatitis B. *BMC Gastroenterol.* **14**, 145. <https://doi.org/10.1186/1471-230X-14-145> (2014).
36. Li, Y., Zhu, W., Song, Z., Liang, W. & Zhou, X. Prediction of risk of blood transfusion in patients with cirrhosis. *Eur. J. Gastroenterol. Hepatol.* **37**, 477–482. <https://doi.org/10.1097/MEG.0000000000002904> (2025).
37. Van den Bossche, L. et al. Tauroursodeoxycholic acid protects bile acid homeostasis under inflammatory conditions and dampens crohn's disease-like ileitis. *Lab. Invest.* **97**, 519–529. <https://doi.org/10.1038/labinvest.2017.6> (2017).
38. Aslan, M. et al. Effect of Tauroursodeoxycholic acid on PUFA levels and inflammation in an animal and cell model of hepatic Endoplasmic reticulum stress. *Hum. Exp. Toxicol.* **37**, 803–816. <https://doi.org/10.1177/0960327117734621> (2018).
39. Xu, X. et al. Tauroursodeoxycholic acid alleviates hepatic ischemia reperfusion injury by suppressing the function of Kupffer cells in mice. *Biomed. Pharmacother.* **106**, 1271–1281. <https://doi.org/10.1016/j.biopha.2018.06.046> (2018).
40. Padia, G. et al. Cystatin C and interleukin-6 for prognosticating patients with acute decompensation of cirrhosis. *JGH Open.* **5**, 459–464. <https://doi.org/10.1002/jgh3.12516> (2021).
41. Haines, R. W. et al. Comparison of Cystatin C and creatinine in the assessment of measured kidney function during critical illness. *Clin. J. Am. Soc. Nephrol.* **18**, 997–1005. <https://doi.org/10.2215/CJN.000000000000203> (2023).
42. Markwardt, D. et al. Plasma Cystatin C is a predictor of renal dysfunction, acute-on-chronic liver failure, and mortality in patients with acutely decompensated liver cirrhosis. *Hepatology* **66**, 1232–1241. <https://doi.org/10.1002/hep.29290> (2017).
43. Wu, J., Wu, Q., Wu, M. & Mao, W. Serum Cystatin C predicts mortality in HBV-Related decompensated cirrhosis. *Biomed. Res. Int.* **2019** (7272045). <https://doi.org/10.1155/2019/7272045> (2019).

44. Zheng, H., Liu, H., Hao, A., Zhang, M. & Wang, D. Association between serum Cystatin C and renal injury in patients with chronic hepatitis B. *Med. (Baltim)*. **99**, e21551. <https://doi.org/10.1097/MD.00000000000021551> (2020).
45. Yan, H. et al. Viral entry of hepatitis B and D viruses and bile salts transportation share common molecular determinants on sodium taurocholate cotransporting polypeptide. *J. Virol.* **88**, 3273–3284. <https://doi.org/10.1128/JVI.03478-13> (2014).
46. Oehler, N. et al. Binding of hepatitis B virus to its cellular receptor alters the expression profile of genes of bile acid metabolism. *Hepatology* **60**, 1483–1493. <https://doi.org/10.1002/hep.27159> (2014).
47. Lefebvre, P., Cariou, B., Lien, F., Kuipers, F. & Staels, B. Role of bile acids and bile acid receptors in metabolic regulation. *Physiol. Rev.* **89**, 147–191. <https://doi.org/10.1152/physrev.00010.2008> (2009).
48. Bertolini, A., Fiorotto, R. & Strazzabosco, M. Bile acids and their receptors: modulators and therapeutic targets in liver inflammation. *Semin Immunopathol.* **44**, 547–564. <https://doi.org/10.1007/s00281-022-00935-7> (2022).
49. Wang, Y. et al. The role of sphingosine 1-phosphate receptor 2 in bile-acid-induced cholangiocyte proliferation and cholestasis-induced liver injury in mice. *Hepatology* **65**, 2005–2018. <https://doi.org/10.1002/hep.29076> (2017).
50. Cepero-Donates, Y. et al. Interleukin-15-mediated inflammation promotes non-alcoholic fatty liver disease. *Cytokine* **82**, 102–111. <https://doi.org/10.1016/j.cyto.2016.01.020> (2016).
51. Jiao, J. et al. Interleukin-15 receptor alpha on hepatic stellate cells regulates hepatic fibrogenesis in mice. *J. Hepatol.* **65**, 344–353. <https://doi.org/10.1016/j.jhep.2016.04.020> (2016).
52. Kong, X. et al. Interleukin-22 induces hepatic stellate cell senescence and restricts liver fibrosis in mice. *Hepatology* **56**, 1150–1159. <https://doi.org/10.1002/hep.25744> (2012).
53. Meng, F. et al. Interleukin-17 signaling in inflammatory, Kupffer cells, and hepatic stellate cells exacerbates liver fibrosis in mice. *Gastroenterology* **143**, 765–776 e763, (2012). <https://doi.org/10.1053/j.gastro.2012.05.049>
54. Li, L., Liu, C., Mao, W., Tumen, B. & Li, P. Taurochenodeoxycholic acid inhibited AP-1 activation via stimulating glucocorticoid receptor. *Molecules* **24** <https://doi.org/10.3390/molecules24244513> (2019).

## Acknowledgements

We would like to express our sincere gratitude to Cheng Yang and Yuan Hu for their technical assistance in flow cytometry analysis.

## Author contributions

H.L. contributed to conceptualization, funding acquisition, formal analysis, software analysis, data curation, and writing. J.Z. and L.W. were involved in methodology, investigation, software analysis, writing and editing. H.X., W.L., and N.S. performed data curation and data validation. J.Z. and L.W. made equal contributions to this study. All authors reviewed the manuscript.

## Declarations

### Competing interests

The authors declare no competing interests.

### Ethical committee and informed consent

According to the 1975 Declaration of Helsinki, this study was approved by an ethic review performed by the Ethics Committee of The First Affiliated Hospital of Chongqing Medical University (Approval No.2020–841). All the patients provided written informed consent prior to being included in the study.

### Consent for publication

All authors have approved the manuscript and agree with its submission.

### Additional information

**Supplementary Information** The online version contains supplementary material available at <https://doi.org/10.1038/s41598-025-16348-z>.

**Correspondence** and requests for materials should be addressed to H.L.

**Reprints and permissions information** is available at [www.nature.com/reprints](http://www.nature.com/reprints).

**Publisher's note** Springer Nature remains neutral with regard to jurisdictional claims in published maps and institutional affiliations.

**Open Access** This article is licensed under a Creative Commons Attribution-NonCommercial-NoDerivatives 4.0 International License, which permits any non-commercial use, sharing, distribution and reproduction in any medium or format, as long as you give appropriate credit to the original author(s) and the source, provide a link to the Creative Commons licence, and indicate if you modified the licensed material. You do not have permission under this licence to share adapted material derived from this article or parts of it. The images or other third party material in this article are included in the article's Creative Commons licence, unless indicated otherwise in a credit line to the material. If material is not included in the article's Creative Commons licence and your intended use is not permitted by statutory regulation or exceeds the permitted use, you will need to obtain permission directly from the copyright holder. To view a copy of this licence, visit <http://creativecommons.org/licenses/by-nc-nd/4.0/>.

© The Author(s) 2025